Acta Crystallographica Section D
Biological Crystallography
ISSN 0907-4449

Crystals of ternary protein–DNA complexes composed of DNA-binding domains of c-Myb or v-Myb, C/EBPα or C/EBPβ and *tom-1*A promoter fragment

Tahir H. Tahirov,[a,b,c]* Motoko Sasaki,[a,b,c] Taiko Inoue-Bungo,[a,b] Atsushi Fujikawa,[a,d] Ko Sato,[a,e] Takashi Kumasaka,[f] Masaki Yamamoto[f] and Kazuhiro Ogata[a,b,c,e]

[a]Kanagawa Academy of Science and Technology (KAST), Yokohama City University School of Medicine, 3-9 Fukuura, Kanazawa-ku, Yokohama 236-0004, Japan, [b]Department of Structural Biology, Yokohama City University School of Medicine, 3-9 Fukuura, Kanazawa-ku, Yokohama 236-0004, Japan, [c]Bio-Crystallography Technology Division, RIKEN Harima Institute, 1-1-1 Kouto, Mikazuki, Sayo, Hyogo 679-5148, Japan, [d]Department of Urology, Yokohama City University School of Medicine, 3-9 Fukuura, Kanazawa-ku, Yokohama 236-0004, Japan, [e]Department of Biochemistry, Yokohama City University School of Medicine, 3-9 Fukuura, Kanazawa-ku, Yokohama 236-0004, Japan, and [f]Structural Biophysics Laboratory, RIKEN Harima Institute, 1-1-1 Kouto, Mikazuki, Sayo, Hyogo 679-5148, Japan

Correspondence e-mail: tahir@med.yokohama-cu.ac.jp

Received 19 March 2001
Accepted 16 July 2001

c-Myb and the C/EBP family are transcriptional regulatory factors that act in concert to regulate the expression of myeloid-specific genes. v-Myb encoded by avian myeloblastosis virus (AMV) is a mutated form of c-Myb that contains point mutations which disrupt the cooperation with C/EBPs. To understand the mechanism of the transcriptional synergy between c-Myb and C/EBPs and the effect of the v-Myb mutations on that synergy, knowledge based on their three-dimensional structures is essential. Crystals of ternary complexes, in which various combinations of the DNA-binding domains of c-Myb or v-Myb and C/EBPα or C/EBPβ are bound to a DNA fragment from *tom-1*A promoter, were obtained by the vapour-diffusion method. Complete diffraction data sets were obtained from each native crystal and two types of iodine-derivative crystals. A three-wavelength MAD data set was also obtained from a bromine-derivative crystal.

1. Introduction

The c-*myb* proto-oncogene product (c-Myb) is a regulator of hematopoietic cell proliferation and differentiation (Oh & Reddy, 1999); whereas it is required for proliferation of immature haematopoietic cells, its expression is suppressed during differentiation. c-Myb activates transcription of a variety of genes by binding to 5′-AACNG-3′ sequences in their promoter regions (Biedenkapp *et al.*, 1988; Weston & Bishop, 1989; Ness *et al.*, 1989; Sakura *et al.*, 1989; Tanikawa *et al.*, 1993). In addition, the promoters of genes targeted by c-Myb often contain binding sites for members of the C/EBP subgroup of the basic region-leucine zipper (bZip) family of transcriptional regulatory factors. For instance, myelomonocyte-specific genes, including *mim-1* (Ness *et al.*, 1989, 1993; Burk *et al.*, 1997), lysozyme (Ness *et al.*, 1993) and *tom-1*A (Burk *et al.*, 1997), as well as the recombination activating genes *RAG1* and *RAG2* (Fong *et al.*, 2000), contain both c-Myb and C/EBP binding sites and their expression is activated cooperatively by the two transcriptional activators. Furthermore, ectopic expression of both Myb and C/EBPβ in erythroid cells and fibroblasts is sufficient to induce endogenous marker genes of myeloid differentiation (Ness *et al.*, 1993).

Two viral forms of Myb (v-Myb) encoded by avian myeloblastosis virus (AMV) and E26 virus are also known (Lipsick & Wang, 1999). AMV v-Myb is a mutant form containing point mutations in its DNA-binding domain that prevent the activation of *mim-1*, whereas E26 v-Myb contains no such mutations and is thus able to activate *mim-1* (Introna *et al.*, 1990). To better understand the mechanism for the synergy between Myb and C/EBPs, we crystallized ternary complexes comprised of the DNA-binding domains of c-Myb or AMV v-Myb and C/EBPα or C/EBPβ bound to the DNA fragments from the chicken *tom-1*A promoter.

2. Experimental procedures

2.1. Protein expression and purification

Polypeptide fragments containing the DNA-binding domains from mouse c-Myb (residues 1–209 or 37–193) or AMV v-Myb (residues 1–128) were overexpressed in *Escherichia coli* BL21(DE3) using a T7 expression system. The bacterial cells containing the overexpressed proteins were harvested, lysed with a French press and centrifuged. The resultant supernatants, each containing the c-Myb or AMV v-Myb protein, were purified through three column-chromatographic steps using phosphocellulose P11 (Whatman International Ltd, England), CM cellulose CM52 (Whatman International Ltd, England) and phenyl Sepharose HP (Amersham Pharmacia Biotech, USA) columns.

Polypeptide fragments containing the DNA-binding domains from rat C/EBPα (residues 268–347) and human C/EBPβ (residues 273–

336 and 259–336) were overexpressed in the same manner as the Myb fragments. In this case, the supernatants, each containing the C/EBPα or C/EBPβ protein, were purified through three column-chromatographic steps using P11, CM52 and Superdex 75 (Amersham Pharmacia Biotech, USA) columns.

2.2. DNA syntheses and purification

The oligonucleotide strands (referred to as DNA, DNA-Br, DNA-I1 and DNA-I2) shown below (where B is 5-bromo-dU and I is 5-iodo-dU) were purchased from Life Technologies Asia Pacific Inc. (Yokohama), purified by reverse-phase HPLC using a Wakosil-DNA column (Wako Pure Chemical Industries Ltd, Osaka) and annealed. The double-stranded DNAs obtained were then separated from the single-stranded material using a hydroxyapatite column (Bio-Rad Laboratories, CA, USA).

DNA
GATGTGGCGCAATCCTTAACGGACTG
TACACCGCGTTAGGAATTGCCTGACC

DNA-Br
GATGBGGCGCAABCCBBAACGGACTG
TACACCGCGBBAGGAABBGCCBGACC

DNA-I1
GATGTGGCGCAATCCITAACGGACTG
TACACCGCGITAGGAATIGCCTGACC

DNA-I2
GATGTGGCGCAATCCTTAACGGACTG
TACACCGCGITAGGAATIGCCTGACC

2.3. Protein–DNA complex preparations

Solutions, each containing one of the following complexes, v-Myb(residues 1–128)–C/EBPβ(259–336)–DNA, c-Myb(35–193)–C/EBPβ(259–336)–DNA, c-Myb(35–193)–C/EBPβ(259–336)–DNA-Br, c-Myb(35–193)–C/EBPβ(259–336)–DNA-I1, c-Myb(35–193)–C/EBPβ(259–336)–DNA-I2, c-Myb(35–193)–C/EBPα(268–347)–DNA, c-Myb(35–193)–C/EBPβ(273–336)–DNA and c-Myb (1–209)–C/EBPβ(273–336)–DNA – hereafter referred to as complexes 1, 2, 2-Br, 2-I1, 2-I2, 3, 4 and 5, respectively – were prepared by first mixing equimolar amounts of each component with 10 m*M* dithiothreitol under salt-free conditions at pH 6.8 and then adding a 10% excess of DNA. Their complex formations were monitored by electrophoresis and the concentrations of the prepared complexes ranged from 6.5–7.5 mg ml^{-1}. The complex-containing solutions were then stored at a temperature of 253 K.

2.4. Crystallization

Crystallization trials were conducted at 297 K in 24-well plates using the sitting-drop vapour-diffusion method. Initial screenings were carried out using Natrix, a crystallization reagent kit for nucleic acids supplied by Hampton Research (Scott *et al.*, 1995), although 12 conditions with high salt concentrations were excluded from the original screening. In all experiments, 2–3 µl drops of protein–DNA complex solution were mixed with 2.5 µl of reservoir solution and equilibrated against 0.5 ml of reservoir solution. The solutions that produced complex crystals were further optimized (Table 1). All the crystals grew in the form of well shaped prisms and grew within 3–5 d to dimensions ranging from 0.3 × 0.1 × 0.1 mm to 1.5 × 0.6 × 0.4 mm. The protein contents of crystals were verified by SDS–PAGE (data not shown). The DNA content of crystals was confirmed by inspection of the X-ray diffraction images, each of which exhibited a diffuse pattern at a resolution of about 3.2 Å (Fig. 1) characteristic of the diffraction of DNA-containing crystals.

Table 1
Composition of reservoir solutions for crystallization of complexes 1–5 and cryoprotectant solutions for flash-cooling of obtained crystals.

Complex	Salt	Buffer	Precipitant	Additive
Crystallization				
1	0.04 *M* $MgCl_2$	0.05 *M* Na cacodylate pH 6.0	20%(*v*/*v*) MPD	None
2, 2-Br, 2-I1, 2-I2	0.05 *M* NH_4 acetate, 0.01 *M* $MgCl_2$	0.05 *M* Tris–HCl pH 7.5	10%(*v*/*v*) MPD	6%(*v*/*v*) glycerol
3	0.1 *M* KCl, 0.005 *M* $MgSO_4$	0.05 *M* Na HEPES pH 7.0	15%(*v*/*v*) MPD	6%(*v*/*v*) glycerol
4	0.1 *M* KCl, 0.005 *M* $MgSO_4$	0.05 *M* Na HEPES pH 7.0	4%(*v*/*v*) MPD	6%(*v*/*v*) glycerol
5-1	0.1 *M* NH_4 acetate, 0.02 *M* $MgCl_2$	0.05 *M* Na HEPES pH 7.0	3.5–4%(*w*/*v*) PEG 8K	6%(*v*/*v*) glycerol
5-2	0.1 *M* KCl, 0.01 *M* $CaCl_2$	0.05 *M* Na HEPES pH 7.0	3.5–4%(*v*/*v*) PEG 400	None
Cryoprotection				
1	None	0.01 *M* Na cacodylate pH 6.0	26%(*v*/*v*) MPD	None
2, 2-Br, 2-I1, 2-I2	0.02 *M* NH_4 acetate, 0.01 *M* $MgCl_2$	0.05 *M* Tris–HCl pH 7.5	10%(*v*/*v*) MPD	6%(*v*/*v*) glycerol, 20%(*v*/*v*) ethylene glycol
3	0.1 *M* KCl, 0.005 *M* $MgSO_4$	0.05 *M* Na HEPES pH 7.0	24%(*v*/*v*) MPD	6%(*v*/*v*) glycerol
4	0.1 *M* KCl, 0.005 *M* $MgSO_4$	0.05 *M* Na HEPES pH 7.0	15%(*v*/*v*) MPD	12%(*v*/*v*) glycerol, 5%(*w*/*v*) PEG 8K
5-1	0.1 *M* NH_4 acetate, 0.02 *M* $MgCl_2$	0.05 *M* Na HEPES pH 7.0	6%(*w*/*v*) PEG 8K	6%(*v*/*v*) glycerol, 24%(*v*/*v*) MPD
5-2	0.1 *M* KCl, 0.01 *M* $CaCl_2$	0.05 *M* Na HEPES pH 7.0	30%(*v*/*v*) PEG 400	None

2.5. Data collection

The characteristics of the crystals were first checked using our laboratory X-ray equipment from MAC Science. X-rays were generated by a self-rotating Cu anode (focus size 0.2 × 2 mm; collimator 0.3 mm) that was powered by an M06XHF^{22}-Fine generator operated at 50 kV and 50 mA, nickel-filtered and focused with a double-mirror; the diffraction from each crystal was recorded on a DIP2030 imaging plate. For data collection at room temperature (293 K) the crystals were mounted in glass capillaries; for data collection at cryotemperature (100 K) the crystals were cryoprotected by soaking them in solutions in which the concentration of cryoprotectant was gradually increased over a period of 3–10 min, mounted in nylon loops supplied by Hampton Research and flash-cooled in a stream of cold nitrogen gas. The final compositions of the best cryoprotectant solutions are listed in Table 1.

Complete data sets were collected from flash-cooled crystals at a temperature of 100 K using synchrotron radiation at SPring-8 beamline BL45XU with an R-AXIS IV imaging plate. The MAD data was collected from a single crystal using a trichromatic concept (Yamamoto *et al.*, 1998). The intensity data were indexed, integrated and scaled using *DENZO* (Otwinowski, 1993) and *SCALEPACK* (Otwinowski & Minor, 1997) software. Details of the data collection, crystal parameters and data-processing statistics are summarized in Table 2.

3. Results and discussion

Crystals of complexes 1–5 diffracted to resolutions of 3 Å or higher (Fig. 1), although the intensities of reflections beyond a resolution of 3.1 Å were signifi-

Table 2
Crystal parameters and data-collection statistics.

Complex	1	2	2-Br	2-Br	2-Br	2-I1	2-I2	3	4	5-1	5-2
Crystal type	Native	Native	Deriv.	Deriv.	Deriv.	Deriv.	Deriv.	Native	Native	Native1	Native2
a (Å)	109.9 (3)	41.7 (3)	41.5 (2)	41.5 (2)	41.5 (3)	41.5 (3)	41.6 (4)	63.2 (5)	62.7 (3)	62.3 (4)	63.1 (3)
b (Å)	166.7 (3)	157.0 (6)	157.2 (6)	157.2 (6)	157 (1)	157.1 (9)	157 (1)	159.6 (9)	73.4 (3)	71.7 (4)	71.6 (4)
c (Å)	39.60 (9)	55.9 (3)	55.2 (4)	55.2 (4)	55.2 (5)	55.6 (3)	55.5 (6)	69.9 (6)	161.7 (5)	160.6 (7)	161.7 (6)
β (°)	90.0	100.2 (2)	100.1 (2)	100.1 (2)	100.1 (3)	100.3 (2)	100.3 (2)	97.7 (4)	90.0	90.0	90.0
Space group	$P2_12_12$	$P2_1$	$P2_1$	$P2_1$	$P2_1$	$P2_1$	$P2_1$	$P2_1$	$P2_12_12_1$	$P2_12_12_1$	$P2_12_12_1$
Z	4	2	2	2	2	2	2	2	4	4	4
Solvent content (%)	65.0	62.3	61.3	61.3	61.3	61.6	61.7	61.1	65.5	60.3	61.0
Wavelength (Å)	1.0200	0.97934	1.0200	0.9197	0.9191	0.9195	0.97934	1.0200	1.0400	1.0200	1.0200
Resolution (Å)	20–2.1	20–2.7	20–3	20–3	20–3	20–2.9	20–2.7	20–3	20–2.45	20–2.6	20–2.4
Last shell	2.17–2.1	2.8–2.7	3.11–3	3.15–3.04	3.11–3	3.0–2.9	2.8–2.7	3.05–3	2.54–2.45	2.64–2.6	2.44–2.4
Observations	162864	58631	41537	40671	38859	38259	57964	67003	205777	112967	132902
Unique reflections	42104	18605	13279	13170	13051	14141	18263	24291	27451	22300	29092
Completeness (%)	97.3	96.0	97.5	96.7	96.0	93.4	96.8	88.7	99.0	97.6	96.7
Last shell	94.2	87.8	92.0	89.0	87.1	84.3	91.7	68.9	95.5	91.5	90.8
R_{sym}	0.069	0.046	0.054	0.056	0.065	0.045	0.050	0.056	0.072	0.053	0.50
Last shell	0.389	0.233	0.191	0.222	0.246	0.217	0.230	0.278	0.397	0.301	0.323
$I/\sigma(I)$	23.9	25.3	19.8	17.6	16.0	22.5	24.1	15.4	27.5	25.4	24.1
Last shell	1.8	2.1	3.0	2.2	1.8	2.2	2.0	2.2	2.2	1.8	2.0

cantly weak. The diffraction was also highly anisotropic for crystals of complex 3. The solvent-content calculation (Matthews, 1968) (Table 2) suggested that crystals of complex 3 contained two molecules in the asymmetric unit, whereas crystals of complexes 1, 2, 4 and 5 contained one molecule in the asymmetric unit. The unit-cell parameters of crystals of complexes 4 and 5 varied only slightly (Table 2), indicating that N- and C-terminal extensions of the c-Myb R1R2R3 domain had little or no effect on crystal packing.

The DNA fragment used for the crystallization of complexes 1–5 was designed such

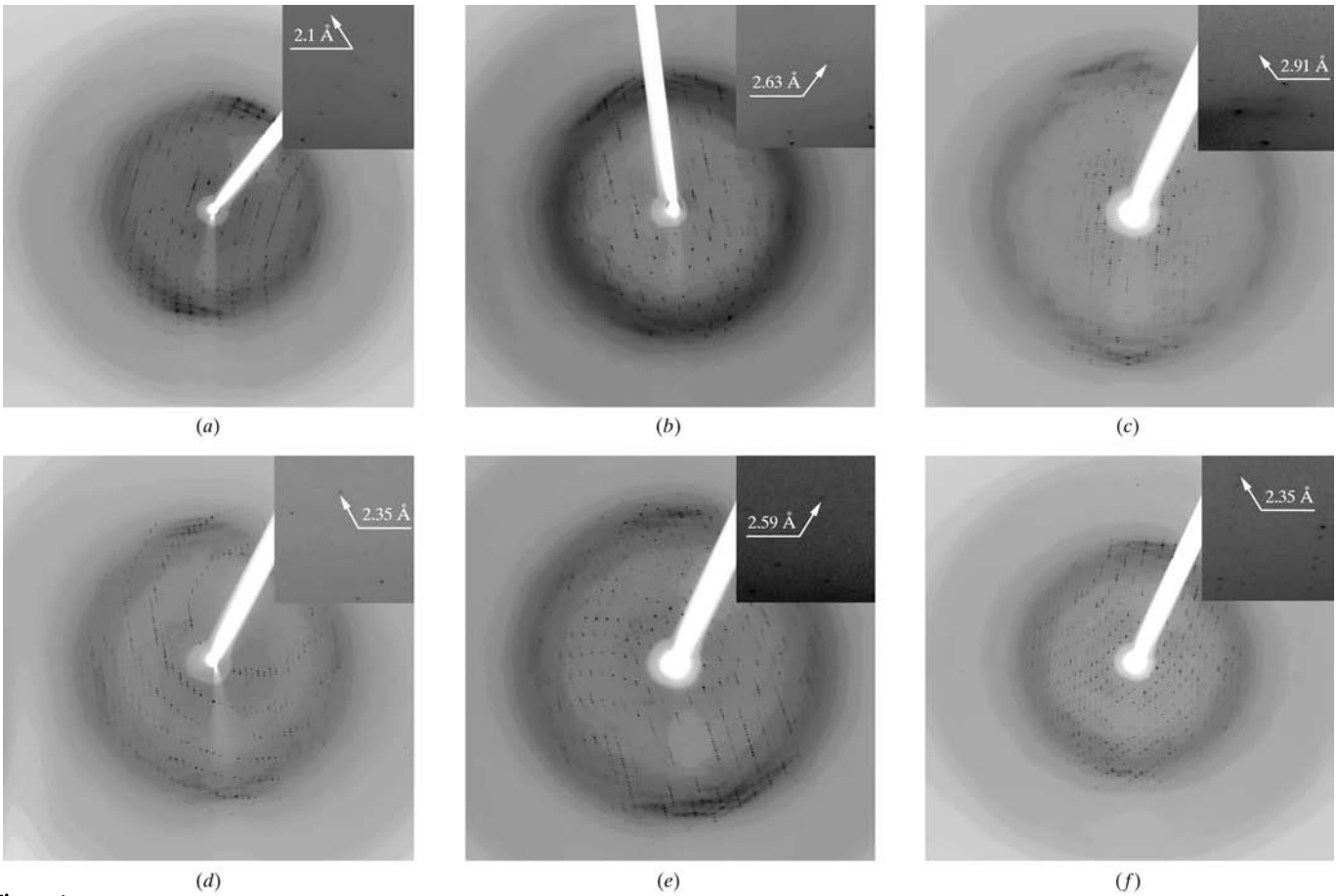

Figure 1
Photomicrographs of crystals of complexes 1 (*a*), 2 (*b*), 3 (*c*), 4 (*d*), 5-1 (*e*) and 5-2 (*f*). The images were recorded at a wavelength of 1.02 Å, a crystal-to-detector distance of 240 mm and an oscillation angle of 1° (*a*); 0.97934 Å, 300 mm and 1.5° (*b*); 1.02 Å, 340 mm and 1° (*c*); 1.04 Å, 300 mm and 1° (*d*); 1.02 Å, 340 mm and 1° (*e*); 1.02 Å, 260 mm and 1° (*f*).

that the DNAs would be paired with overhanging bases to form continuous double-stranded B-DNA pseudo-helices in which contiguous complex molecules were related by crystallographic or pseudo-twofold screw symmetry. If two consecutive DNA fragments were connected *via* the overhanging G and C bases, as expected, then the calculated length of the connected 52 bp B-DNA would be 176.8 Å, based on an axial rise of 3.4 Å. With the reduction in temperature from 297 to 100 K, however, the crystals of the complexes shrank approximately 5 Å along the longest axis of the unit cell (data not shown). Thus, if the DNA molecules were packed alongside the longest axis of the unit cell, it would be expected that the length of the 52 bp B-DNA would be reduced at cryotemperature to approximately 172 Å. However, for each crystal of the c-Myb-containing complexes, the longest axis of the unit cell was shorter than 172 Å, ranging from 157.0 to 161.7 Å, while the corresponding value was 166.7 Å for crystals of v-Myb-containing complexes (Table 2). Several factors may account for the unit cell axis being shorter than the typical length of the 52 bp B-DNA: the DNA may have been bent or distorted from the ideal B-form structure, the DNA pseudo-helix may have formed along the unit-cell diagonals or the molecules may have been discretely packing without formation of a continuous DNA pseudo-helix.

Determination of the crystal structures of complexes 1–5 using MIR, MAD and molecular-replacement methods is complete and will be discussed elsewhere.

We thank S. Akira for NF-IL6 cDNA, S. Ishii for helpful discussions and generous support and T. Kato and M. Hosaka for generous support. This research was supported in part by CREST (Core Research for Evolutional Science and Technology) of the Japan Science and Technology Corporation (JST) to KO.

References

Biedenkapp, H., Borgmeyer, U., Sippel, A. E. & Klempnauer, K.-H. (1988). *Nature (London)*, **335**, 835–837.

Burk, O., Worpenberg, S., Haenig, B. & Klempnauer, K.-H. (1997). *EMBO J.* **16**, 1371–1380.

Fong, I. C., Zarrin, A. A., Wu, G. E. & Berinstein, N. L. (2000). *Mol. Immunol.* **37**, 391–402.

Introna, M., Golay, J., Frampton, J., Nakano, T., Ness, S. A. & Graf, T. (1990). *Cell*, **63**, 1287–1297.

Lipsick, J. S. & Wang, D.-M. (1999). *Oncogene*, **18**, 3047–3055.

Matthews, B. W. (1968). *J. Mol. Biol.* **33**, 491–497.

Ness, S. A., Kowenz-Leutz, E., Casini, T., Graf, T. & Leutz, A. (1993). *Genes Dev.* **7**, 749–759.

Ness, S. A., Marknell, A. & Graf, T. (1989). *Cell*, **59**, 1115–1125.

Oh, I. H. & Reddy, E. P. (1999). *Oncogene*, **18,** 3017–3033.

Otwinowski, Z. (1993). *DENZO. An Oscillation Data Processing Suite for Macromolecular Crystallography.* Yale University, New Haven, CT, USA.

Otwinowski, Z. & Minor, W. (1997). *Methods Enzymol.* **276**, 307–326.

Sakura, H., Kanei-Ishii, C., Nagase, T., Nakagoshi, H., Gonda, T. J. & Ishii, S. (1989). *Proc. Natl Acad. Sci. USA*, **86**, 5758–5762.

Scott, W. G., Finch, J. T., Grenfell, R., Fogg, J., Smith, T., Gait, M. J. & Klug, A. (1995). *J. Mol. Biol.* **250**, 327–332.

Tanikawa, J., Yasukawa, T., Enari, M., Ogata, K., Nishimura, Y., Ishii, S. & Sarai, A. (1993). *Proc. Natl Acad. Sci. USA*, **90**, 9320–9324.

Weston, K. & Bishop, J. M. (1989). *Cell*, **58**, 85–93.

Yamamoto, M., Kumasaka, T., Fujisawa, T. & Ueki, T. (1998). *J. Synchrotron Rad.* **5**, 222–226.